Scientific Research Publishing

Journal of Modern Physics, 2020, 11, 967-975
https://www.scirp.org/journal/jmp
ISSN Online: 2153-120X
ISSN Print: 2153-1196

On the Ratios Dark Matter (Energy)/Ordinary Matter ≈ 5.4(13.6) in the Universe

F. C. Hoh

Retired, Dragarbrunnsg. 55C, Uppsala, Sweden
Email: hoh@telia.com

How to cite this paper: Hoh, F.C. (2020) On the Ratios Dark Matter (Energy)/Ordinary Matter ≈ 5.4(13.6) in the Universe. *Journal of Modern Physics*, **11**, 967-975.
https://doi.org/10.4236/jmp.2020.117060

Received: June 5, 2020
Accepted: June 27, 2020
Published: June 30, 2020

Abstract

An upper limit of the average ratio dark matter/ordinary matter in galaxies is estimated to be 8.4, in agreement with the observed ratio 5.4. Upper limit of the average ratio dark energy/ordinary matter for slowly moving protons in the outer parts of the universe is estimated to be 8.4, much less than the observed ratio 13.6. The discrepancy is tentatively attributed to that the bulk of the protons in these outer parts of the universe moves fastly and their contribution to dark energy has not been estimated. The positive and negative relative energies between the diquark and quark in the proton play the roles of dark energy and dark matter, respectively.

Keywords

Relative Energy Between Quarks, Scalar Strong Interaction Hadron Theory, Ratio of Dark Matter to Ordinary Matter, Ratio of Dark Energy to Ordinary Matter, Gravitational Pull of Diquark and Quark, Proton Orbit, Diquark Equations

1. Introduction

The mass-energy density of the dominant cosmic constituents averaged over the entire universe is [1]

$$\text{Dark energy: Dark matter: Ordinary matter} \approx 68\%:27\%:5\% \tag{1.1}$$

Dark energy and dark matter has been interpreted to be the positive and negative, respectively, relative energy between the diquark *uu* and the quark *d* in the protons in the hydrogen gas permeating the universe [2]. Subsequently [3], the negative relative energy has been used to account for the galaxy rotation curve instead of the unobserved dark matter. The positive relative energy has been used to account for the acceleratingly expanding universe instead of the unobserved dark energy. Further, by including the negative relative energy, a neutron

star with a mass near the Tolman-Oppenheimer-Volkoff limit M_{TOV} ~3 solar masses is prevented from collapsing into a gravitational singularity but becomes a "black neutron star".

These qualitative results however do not shed any light on the observed ratios in (1.1). The purpose of this paper is to extend [3] to provide some quantitative estimates on the limits on these ratios (1.1). The proton size is calculated in Section 2. In Section 3, the hydrogen atom structure is illustrated. Section 4 shows the proton structure and estimated upper limits of the ratio "dark matter"/ordinary matter in galaxies. Analogous estimates of "dark energy"/nonrelativistic ordinary matter in a small part of the outer part of the universe are given. In the **Appendix**, gravitational effects are included. Equations of motion for a diquark are constructed. When combined with the equations of motion for a quark, equations of motion for a diquark-quark baryon obtained earlier are recovered.

2. Proton Wave Functions and Its Size

As in [3] [4], the scalar strong interaction hadron theory (SSI) [4] provides the framework. Parts of Sections 2 - 5 in [3] are reproduced for use here together with an extension. Let a *uu* diquark A at x_I interact with a d quark B at x_{II} via a scalar interaction $V_{AB}(x_I, x_{II})$. Since the quarks are not observable, introduce the proton coordinate X_p and the relative coordinate x,

$$x^\mu = x_{II}^\mu - x_I^\mu, \quad X_p^\mu = (1-a_m)x_I^\mu + a_m x_{II}^\mu \tag{2.1}$$

where a_m is an arbitrary real constant. The laboratory coordinate X_p is an observable but x is not but "hidden". The total proton wave function is of the form [3 (3.2)],

$$\begin{aligned} \chi_{0\dot{b}}(x_I, x_{II}) &= \chi_{0\dot{b}}(\underline{x})\exp\left(-iK_\mu X_p^\mu + i\omega_K x^0\right) \\ \psi_0^a(x_I, x_{II}) &= \psi_0^a(\underline{x})\exp\left(-iK_\mu X_p^\mu + i\omega_K x^0\right) \end{aligned} \tag{2.2}$$

$$K_\mu = (E_K, -\underline{K}) \tag{2.3}$$

Here, a, $\dot{b}$ run from 1 to 2. In the rest frame considered in [4], $\underline{K} = 0$, E_0 is the proton mass and $-\omega_0$ is the relative energy between *uu* and *d*.

Equation (1.3) is governed by the baryon wave equations [3 (2.3)] which contains the derivatives $\partial_I^{a\dot{b}}$ and $\partial_{II\dot{e}f}$ with respect to x_I and x_{II}, respectively, appear. For the present case, these derivatives leads to the same result [3 (5.1)] for

$$a_m = \frac{1}{2} + \frac{\omega_0}{E_0} \tag{2.4}$$

[3 (5.2)]. Since a_m can range from $-\infty$ to $+\infty$, the relative energy $-\omega_0$ can likewise do so. This provides the basis of the results in [3].

$\chi_0(\underline{x})$ and $\psi_0(\underline{x})$ in (1.3) have been decomposed into an angular part and a radial part $g_0(r)$ and $f_0(r)$ in [3 (3.4)]. Here, the diquark-quark distance $r = |\underline{x}|$. $g_0(r)$ and $f_0(r)$ have been solved and plotted for neutron in **Figure 1** in [3]. Since the masses of proton and neutron are almost the same, as do those of the u and d quarks, this plot can be used here. Inspection of this figure led to the estimate that the average $r = r_a \approx 4$ fm which has been employed in [3 Sections 6 and 8].

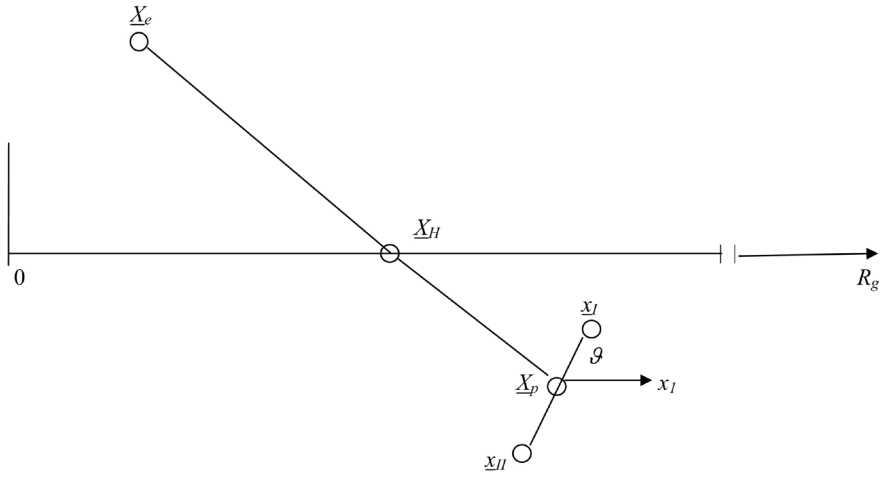

Figure 1. Structure of a rest frame hydrogen atom near the center of a galaxy from which the radius R_g departs. $\underline{X}_e$ denotes the electron coordinate in this laboratory frame, $\underline{X}_p$ that of the proton and $\underline{X}_H$ their center of mass or hydrogen atom. For illustration, the proton-electron mass ratio m_p/m_e has been deliberately lowered to about 2 so that $\underline{X}_e$ falls within the figure. The diquark *uu* is at $\underline{x}_I$ and quark *d* at $\underline{x}_{II}$. A "hidden", relative coordinate system $\underline{x} = \underline{x}_{II} - \underline{x}_I = (x_1, x_2, x_3)$ centered at $\underline{X}_p$ is introduced. ϑ denotes the angles in this "hidden" $\underline{x}$ space and is randomly distributed here.

This r_a value may be improved by weighing r with the squares of $\chi_{0\dot{b}}(\underline{x})$ and $\psi_0^a(\underline{x})$ and averaging over the relative space. With the plots in [3], computation yields for the average $r = |\underline{x}|$

$$r_a = \frac{\int \mathrm{d}\underline{x}^3 r\left(\left(\chi_{0\dot{b}}(\underline{x})\right)^* \chi_{0\dot{b}}(\underline{x}) + \left(\psi_0^a(\underline{x})\right)^* \psi_0^a(\underline{x})\right)}{\int \mathrm{d}\underline{x}^3 \left(\left(\chi_{0\dot{b}}(\underline{x})\right)^* \chi_{0\dot{b}}(\underline{x}) + \left(\psi_0^a(\underline{x})\right)^* \psi_0^a(\underline{x})\right)} = \frac{\int \mathrm{d}r r^3 \left(g_0^2(r) + f_0^2(r)\right)}{\int \mathrm{d}r r^2 \left(g_0^2(r) + f_0^2(r)\right)} = 3.23 \text{ fm} \tag{2.5}$$

3. Hydrogen Atom Structure

The structure of the hydrogen atom in the rest frame in SSI is illustrated in **Figure 1**.

The electron cloud is symmetrically concentrated within a sphere with Bohr radius $a_0 \approx 0.53$ Å centered at the center of mass coordinate $\underline{X}_H$. The associated radial wave functions are

$$R_{00}(r_e) \propto \exp(-r_e/a_o), \quad R_{10}(r_e) \propto (2 - r_e/a_o)\exp(-r_e/a_o), \quad r_e = |\underline{X}_e - \underline{X}_H| \tag{3.1}$$

Here, $\underline{X}_e$ is the actual (not scaled down as is illustrated in **Figure 1**) electron coordinate in the observable laboratory frame. R_{00} refers to the ground state and R_{10} to the first radically excited state.

Accompanying this electron cloud is an associated proton cloud likewise symmetrically distributed around $\underline{X}_H$. This cloud is analogously concentrated inside a sphere with the proton Bohr radius

$$a_{0p} = a_0 \left(m_p / m_e \right) = 28.8 \text{ fm} \tag{3.2}$$

The observable mass m_p and charge $+e$ of the proton reside in the laboratory frame proton coordinate $\underline{X}_p$ in Figure 1. The diquark uu and quark d are located at the unobservable coordinates $\underline{x}_I$ and $\underline{x}_{II}$, respectively. $\underline{x}_{II} - \underline{x}_I = \underline{x}$ is the "hidden" unobservable relative space "isolated" from the observable laboratory space $\underline{X}$.

4. Upper Limit of Ratio of Dark Matter to Ordinary Matter in Galaxies

In [3 Section 8], dark matter has been used to account for the galaxy rotation curve qualitatively. Defining the ratio of dark energy/ordinary matter to be R_{DE} and dark matter/ordinary matter to be $-R_{DM}$, (1.1) yields

$$\begin{bmatrix} R_{DE} \\ R_{DM} \end{bmatrix} = -\frac{\omega_0}{E_0} = \begin{bmatrix} 68\%/5\% = 13.6 & \text{for dark energy} \\ -27\%/5\% = -5.4 & \text{for dark matter} \end{bmatrix} \tag{4.1}$$

As the galaxy in Section 3 expands, the hydrogen atom in Figure 1 will move outwards from the galaxy center and becomes far away from it. This has been considered in [3 Section 8]. The constituents of this atom are illustrated in Figure 2.

The outward motion of the atom is due to thermal expansion of the young galaxy containing it and proceeds via Coulomb force between the electrons in the hydrogen gas; the proton gets dragged along. The gravitational pull from matter in the central part of the galaxy on the proton produces a negligible shift of X_p and asymmetry in the proton cloud due to the strong restraining electron-proton Coulomb force. Since the quarks are in the "hidden" relative space and do not interact with the electron in the laboratory space but interact with the ambient gravitational field [3 V_{BG} in (2.1)], [2 end of Section 5], they will be pulled back from X_p by these gravitational forces and lag behind to the left of X_p. Further, the diquark uu at x_I is about twice as heavy as the quark d at x_{II} [4 Table 5.2] and will feel twice the gravitational pull and hence lies closer to the galactic center and to the left of x_{II}, also mentioned below (A6).

Since the proton is largely confined inside the proton Bohr sphere, its constituents, the diquark uu at $\underline{x}_I$ and quark d at $\underline{x}_{II}$, are likewise confined to the same

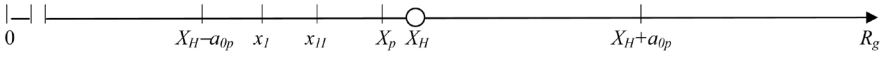

Figure 2. It develops to the right part of Figure 3 in [3]. It illustrates the constituents of the hydrogen atom in Figure 1 moved outwards from the galaxy center to a region far from it. The proton Bohr orbit with radius $a_{0p} \approx 28.8$ fm corresponds to the electron orbit with the Bohr radius $a_0 \approx 0.53$ Å in (3.1). Both are centered at the center of mass X_H which is also the center of the hydrogen atom. The proton cloud is concentrated inside a sphere of radius a_{0p}. This sphere intersects the R_g axis at $X_H \pm a_{0p}$. Here an X_p point to the left of X_H is chosen for consideration; the associated X_e lies far to the right and is not shown. The associated diquark uu is located at x_I and quark d at x_{II} closer to the galactic center $R_g = 0$ due to differential gravitational pull.

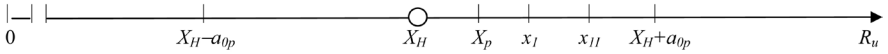

Figure 3. It corresponds to the right part of Figure 4 in [3]. It illustrates the constituents of the hydrogen atom in **Figure 2** moved outwards to an outer region of the universe which is beginning to expand acceleratingly. The horizontal line represents the distance R_u from some unspecified inner region of the universe. The figure has the same form as **Figure 2** but with quarks moved to the right side of the proton coordinate $\underline{X}_p$. The associated $\underline{X}_e$ lies far to the left and is not shown.

proton cloud sphere. This provides a limit $\underline{x}_I \geq X_H - a_{0p}$ in **Figure 2**. The above mentioned symmetry yields an average value $X_p = X_H$. Further, the mean value of $|x_{II} - x_I| = |\underline{x}| = r_a \approx 3.23$ fm in (2.5). Inserting these three relations into (2.1), (2.4) and (4.1) leads to the estimated limit

$$R_{DM} \geq \frac{1}{2} - a_m = \frac{1}{2} - \frac{a_{op}}{r_a} = -8.4 \tag{4.2}$$

consistent with the observed average of −5.4 in (4.1) which lies near the middle of the allowed range 0 to −8.4..

5. Ratios of Dark Energy to Nonrelativistic Ordinary Matter in Outer Parts of Universe

As the hydrogen atom in **Figure 2** continues to move outwards, it enters the outer regions of the universe, as has been considered in [3 Section 9]. In the beginning of this region, the left part of Figure 4 in [3] shows that this hydrogen atom, being too far away from the galaxy's central region, is no longer affected by any gravitational force and reverts from the configuration of **Figure 2** back to that in Figure 3(c) in [3]. This configuration is unstable with respect to dark energy generated and eventually turns into the configuration on the right part of Figure 4 in [3] where the quarks in the proton are being pushed outwards acceleratingly by the increasing dark energy generated in this region. The situation is illustrated in **Figure 3**.

In this region, the protons are expected to move fastly so that the above treatment, valid for rest frame and approximately also for slowly moving protons, no longer holds. The rest frame treatment in [4 Ch.10-12] no longer holds and no result can be reached. However, just before this region is reached, the norelativistic left part of Figure 3 in [3] is approximately applicable so that a treatment analogous to that in section 4 can be carried out. Applying **Figure 3** instead of **Figure 2** with the criterion $\underline{x}_I \geq X_H - a_{0p}$ above (4.2) replaced by $\underline{x}_{II} \leq X_H + a_{0p}$ turns (4.1) to

$$R_{DE} \leq \frac{1}{2} - a_m = \frac{1}{2} + \frac{a_{op} - r_a}{r_a} = 8.4 \tag{5.1}$$

This disagrees with the observed $R_{DE} = 13.6$ in (4.1). This is not surprising in view of the consideration above (5.1); (5.1) holds only for slowly moving protons which constitute only a small part of the protons in **Figure 3**. The bulk of the protons there moves fastly and the rest frame treatment here does not hold.

Conflicts of Interest

The author declares no conflicts of interest regarding the publication of this paper.

References

[1] Wikipedia (2020) https://en.wikipedia.org/wiki/Main_Page

[2] Hoh, F.C. (2019) *Journal of Modern Physics*, **10**, 635-640. https://doi.org/10.4236/jmp.2019.106045

[3] Hoh, F.C. (2019) *Journal of Modern Physics*, **10**, 1645-1658. https://doi.org/10.4236/jmp.2019.1014108

[4] Hoh, F.C. (2019) Scalar Strong Interaction Hadron Theory. II Nova Science Publishers, New York.

Appendix. Inclusion of Gravitation and Equation of Motion for Diquark

The theory SSI [4] underlying the above results does not include gravitation. These results have been obtained by phenomenologically joining gravitation to the baryon sector of SSI. Here, gravitation will be introduced into the equations of motion for quarks, from which a set of somewhat generalized equations of motion for baryons will be constructed. This construction differs somewhat from the one step construction in [4 Ch 9] in that it is divided into two steps. In the first one, equations of motion for diquark are written down. These are then combined with a set of quark equations to form the baryon equations. This is done because diquark plays a decisive role in the above sections.

For the present applications, it is sufficient to introduce a scalar gravitational potential into the quark equations, such $V_{GB}(x_{II})$ in [3 (2.1)],

$$V_{GB}\left(x_{II}\right)=m_B\varepsilon_{II},\quad \varepsilon_{II}=\varepsilon_{II}\left(\left|\underline{x}_{II}\right|\right)=-\frac{GM_g}{\left|\underline{x}_{II}\right|} \tag{A1}$$

Here, G is the gravitational constant, m_B the mass of the d quark B and M_g the mass of the galaxy containing quark B. $\underline{x}_{II}$ is the position of this quark in a coordinate system with its origin at the center of the galaxy denoted by 0 in **Figure 2** above. ε_{II} is typically a small number of the magnitude of $!0^{-6}$ in the middle of the Milky Way. The gravitational force on this quark is thus negligible but not relative to that on the accompanying diquark in (A6) below.

The potential (A1) containing m_B can be moved to the right side of [3 (2.1)] which now reads

$$\partial_{II}^{d\dot{e}}\chi_{B\dot{e}}\left(x_{II}\right)-i\left(V_{BC}\left(x_{II}\right)+V_{BA}\left(x_{II}\right)\right)\psi_B^d\left(x_{II}\right)=im_B\left(1+\varepsilon_{II}\right)\psi_B^d\left(x_{II}\right) \tag{A2.a}$$

$$\partial_{II\,\dot{e}f}\psi_B^f\left(x_{II}\right)-i\left(V_{BC}\left(x_{II}\right)+V_{BA}\left(x_{II}\right)\right)\chi_{B\dot{e}}\left(x_{II}\right)=im_B\left(1+\varepsilon_{II}\right)\chi_{B\dot{e}}\left(x_{II}\right) \tag{A2.b}$$

which has the same form as the starting [4 (9.1.2a, 2b)] with m_B multiplied by $(1+\varepsilon_{II})$.

Potentials corresponding to (A1) are now introduced into the quark equations [4 (9.1.1, 3)] for quark A at x_I and quark C at x_{III}, respectively. These now read

$$\partial_I^{a\dot{b}}\chi_{A\dot{b}}\left(I\right)-i\left(V_{AB}\left(I\right)+V_{AC}\left(I\right)\right)\psi_A^a\left(I\right)=im_A\left(1+\varepsilon_I\right)\psi_A^a\left(I\right) \tag{A3a}$$

$$\partial_{I\,\dot{b}c}\psi_A^c\left(I\right)-i\left(V_{AB}\left(I\right)+V_{AC}\left(I\right)\right)\chi_{A\dot{b}}\left(I\right)=im_A\left(1+\varepsilon_I\right)\chi_{A\dot{b}}\left(I\right) \tag{A3b}$$

$$\partial_{III}^{g\dot{h}}\chi_{C\dot{h}}\left(III\right)-i\left(V_{CA}\left(III\right)+V_{CB}\left(III\right)\right)\psi_C^g\left(III\right)=im_C\left(1+\varepsilon_{III}\right)\psi_C^g\left(III\right) \tag{A4a}$$

$$\partial_{III\,\dot{h}k}\psi_C^k\left(III\right)-i\left(V_{CA}\left(III\right)+V_{CB}\left(III\right)\right)\chi_{C\dot{h}}\left(III\right)=im_C\left(1+\varepsilon_{III}\right)\chi_{C\dot{h}}\left(III\right) \tag{A4b}$$

Following [4 Section 9.2], the V's on the left sides are moved to the right sides and (A3) and (A4) are multiplied together. While wave functions of three quarks were multiplied together and generalized to baryon wave functions in [4], only two quarks A and C are involved here. Analogous to [4 (2.2.2)], the diquark wave functions are

$$\chi_{A\dot{b}}\left(x_I\right)\chi_{C\dot{h}}\left(x_{III}\right)\to\chi_{\{\dot{b}\dot{h}\}}\left(x_I,x_{III}\right)\to\chi_{\{\dot{b}\dot{h}\}}\left(x_I\right) \tag{A5a}$$

$$\psi_A^c(x_I)\psi_C^k(x_{III}) \to \psi^{\{ck\}}(x_I, x_{III}) \to \psi^{\{ck\}}(x_I) \tag{A5b}$$

Here, quarks A and C belong to the same species and are merged together via $C \to A$ and $x_{III} \to x_I$. This leads to $V_{AC} = V_{CA} = 0$. The multiplication and (A5) yields the diquark wave equations

$$\partial_I^{a\dot{b}} \partial_I^{g\dot{h}} \chi_{A\{\dot{b}\dot{h}\}}(x_I) = -\left(V_{AB}^2(\underline{x}_I) + m_A^2(1+\varepsilon_I)^2\right)\psi_A^{\{ag\}}(x_I) \tag{A6a}$$

$$\partial_{I\dot{b}c}\partial_{I\dot{h}k}\psi_{A\{\dot{b}\dot{h}\}}(x_I) = -\left(V_{AB}^2(\underline{x}_I) + m_A^2(1+\varepsilon_I)^2\right)\chi_{A\{\dot{b}\dot{h}\}} \tag{A6b}$$

in which products not formimg diquark have been dropped. Equations (A5) has the same form as the meson wave equations [4 (2.3.22)] in which the quark masses are m_p+m_r in [4 (2.3.27)]. Analogously, the diquark mass here is $2m_A$. The small gravitational pull on the diquark is thus about twice that on the quark mentioned below (A1). This small difference causes, over long time and large distances, the diquark coordinate x_I to lie closer to the galactic center than does the quark coordinate x_{II} in **Figure 2**, as was mentioned there. How this is accomplished has not been investigated.

The potentials equations [4 (9.1.4a, 4c)] are likewise multiplied together to yield

$$\begin{aligned}\overline{\square}_I \overline{\square}_I V_{AB}^2(\underline{x}_I) = \frac{1}{4} g_s^4 \{&\psi_A^{\{ag\}}(x_I)\chi_{A\{ag\}}(x_I) + \psi_A^{\{\dot{a}\dot{g}\}}(x_I)\chi_{A\{\dot{a}\dot{g}\}}(x_I) \\ &+ \psi_B^{\{eh\}}(x_I)\chi_{B\{eh\}}(x_I) + \psi_B^{\{\dot{e}\dot{h}\}}(x_I)\chi_{B\{\dot{e}\dot{h}\}}(x_I)\}\end{aligned} \tag{A7}$$

analogous to [4 (9.2.2, 2.9, 2.11] involving three quarks. The corresponding expression for quark B [4 (9.4.1b)] reads here

$$\overline{\square}_{II} V_{BA}(\underline{x}_{II}) = \frac{1}{2} g_s^2 \{\psi_A^a(x_{II})\chi_{Aa}(x_{II}) + \psi_A^{\dot{a}}(x_{II})\chi_{A\dot{a}}(x_{II})\} \tag{A8}$$

Multiplying together the diquark A equations (A6, A7) and the quark B equations (A2), with the potentials V moved to the right side, and generalized the product wave functions to nonseparable baryon wave functions similar to [4 (9.2.12)] leads to

$$\begin{aligned}&\partial_I^{a\dot{b}}\partial_I^{g\dot{h}}\partial_{II\dot{e}f}\chi_{\{\dot{b}\dot{h}\}}^{\ \ f}(x_I, x_{II}) \\ &= -i\left(m_A^2 m_B(1+\varepsilon_I)^2(1+\varepsilon_{II}) + \Phi_b(\underline{x}_I, \underline{x}_{II})\right)\psi_{\dot{e}}^{\{ag\}}(x_I, x_{II}) \\ &\partial_{I\dot{b}c}\partial_{I\dot{h}k}\partial_{II}^{d\dot{e}}\psi_{\ \dot{e}}^{ck}(x_I, x_{II}) \\ &= -i\left(m_A^2 m_B(1+\varepsilon_I)^2(1+\varepsilon_{II}) + \Phi_b(\underline{x}_I, \underline{x}_{II})\right)\chi_{\dot{b}\dot{h}}^{\ \ d}(x_I, x_{II})\end{aligned} \tag{A9}$$

which reduces to the diquark-quark baryon wave equations [4 (9.2.14)] for $\varepsilon \to 0$. The generalization of quark masses in (A9) to internal mass operators [4 (9.3.8, 13, 14)] operating on internal functions [4 (9.3.1)] is unaffected by inclusion of gravitation.

Multiplying together (A7) and (A8) and using the generalization [4 (9.2.2)] reproduces the baryon potential equation [4 (9.2.11)],

$$\overline{\underline{\quad}}_{I}\overline{\underline{\quad}}_{I}\overline{\underline{\quad}}_{II}\Phi_{b}\left(\underline{x}_{I},\underline{x}_{II}\right)=\frac{1}{4}g_{s}^{6}\left\{\chi_{\{\dot{b}\dot{h}\}}^{f}\left(x_{I},x_{II}\right)\psi^{\{\dot{b}\dot{h}\}}{}_{f}\left(x_{I},x_{II}\right)+c.c.\right\} \quad \text{(A10)}$$